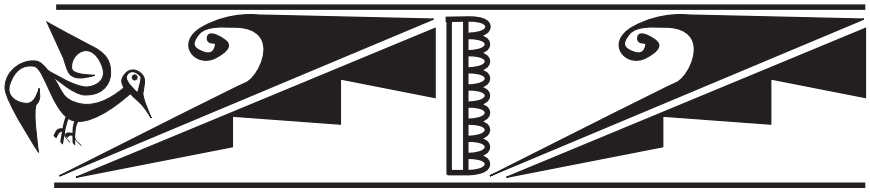

Condensed Matter Physics

Non-Aqueous Chemistry of Uranyl Complexes with Tripodal Ligands

Carol J. Burns,
David L. Clark,
Paul B. Duval,
Brian L. Scott
Los Alamos National Laboratory, Los Alamos, NM 87545, USA

Introduction

The trans dioxo uranyl(VI) ion (UO_{22}^{+}) is remarkably stable with respect to the U=O bond, which dominates the stereochemistry of its coordination compounds in both aqueous and non-aqueous solutions. The linear O=U=O unit directs all other ligands to coordinate in an equatorial plane perpendicular to the O=U=O axis. In aqueous solution, uranyl coordination chemistry has been developed with a wide array of weak-field ligands that coordinate in the equatorial plane. In contrast, non-aqueous uranyl chemistry incorporating stronger donor ligands at equatorial sites has been less well developed. In this paper, the use of tripodal ligands with strong amide and alkoxide donors is employed, with an aim towards probing the electronic and steric effects of these cis-directing ligands on the structure and bonding of the trans dioxo unit.

Description of Work

The synthetic strategy entails two possible routes (Figure 1): (1) metathesis reaction of a uranyl chloride precursor with an alkali metal salt of the ligand; or (2) amine elimination involving a uranyl amido complex and the protonated version of the tripodal ligand. The reactions in step 1 are more prone to complications with respect to reduction of the uranyl center, which are obviated in step 2. The tripodal ligands selected include triamidoamine donors (as shown in Figure 1), calix[4]arenes, and Kläui ligands. Elucidation of the electronic structure and bonding of the products is obtained by a diverse array of characterization techniques, including X-ray diffraction and EXAFS, multinuclear nuclear magnetic resonance (NMR) spectroscopy, infrared (IR) and Raman, luminescence, and optical spectroscopy.

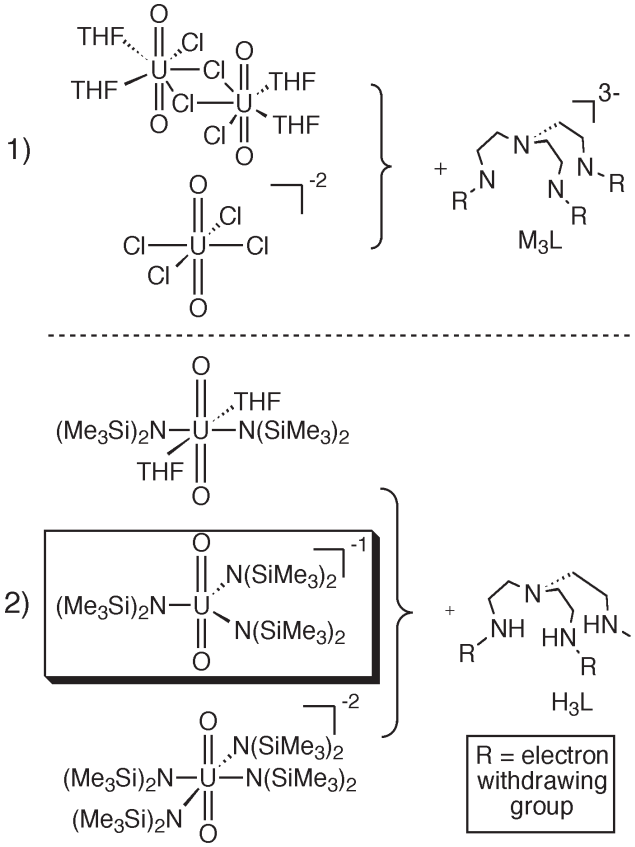

Results

Although amido ligands (NR2)- are prevalent in low-valent uranium chemistry, uranyl amido complexes are exceedingly rare, being restricted to the derivatives shown in Figure 1. The tris(amido) complex shown above has just recently been synthesized in our lab, and is an extremely rare example of a uranyl complex with only three equatorial ligands.

CP532, Plutonium Futures – The Science, edited by K. K. S. Pillay and K. C. Kim,
2000 American Institute of Physics 1-56396-948-3

Despite the inherent coordinative unsaturation, this complex is nevertheless relatively electron-rich, as the addition of a neutral donor ligand to expand the coordination geometry is reversible.

The results obtained from the addition of various tripodal ligands to uranyl species depend primarily on electronic factors associated with the ligand employed. As shown in Figure 2, ligands with electron-withdrawing substituents attached to the amido donors generate no perturbation of the trans dioxo unit on uranium (I). Alternatively, the use of more electron-releasing silyl substituents results in activation of one uranyl oxo group and partial reduction, to give an unprecedented mixed-valent U(V/VI) oxo-imido complex (II). Results from other reactions are evaluated in a similar context.

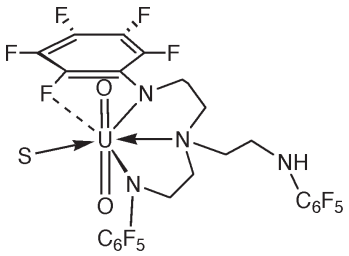

I

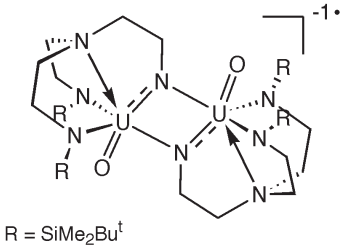

II

Organoactinides—New Type of Catalysts for Carbon-Carbon, Carbon-Nitrogen, and Carbon-Silicon Bond Formations

Moris S. Eisen
Department of Chemistry and Institute of Catalysis Science and Technology, Technion - Israel Institute of Technology, Haifa 32000, Israel

In recent years the catalytic aspects of the organometallic complexes of d^0/f^n-block have attracted major attention and have been in particular the focus of numerous investigations for the functionalization of unsaturated organic molecules. Metal-mediated oligomerization of terminal alkynes is of considerable current interest because it can lead to a variety of organic enynes and oligoacetylene products that are useful synthetic precursors for the synthesis of natural products and also for organic conducting polymers.

We have recently demonstrated that organoactinides complexes of the type $Cp^*_2AnMe_2$ ($Cp^* = C_5Me_5$; An = U, Th) are active catalysts for the linear oligomerization of terminal alkynes and the extent of oligomerization was found to be strongly dependent on the electronic and steric properties of the alkyne substituents. For example, bulky alkynes reacted with high regioselectivity towards dimer and/or trimers (eq. 1), whereas for non-bulky alkynes, the oligomerization yielded dimers to decamers with total lack of regioselectivity.[1] The addition of primary amines, for An = Th, allowed the chemoselective formation of dimers[2] whereas for An = U the hydroamination product was obtained (eq. 2).[3]

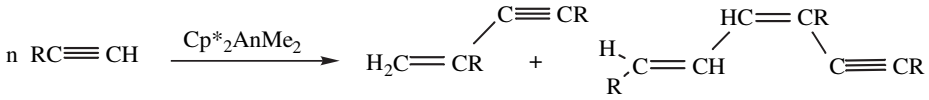

(1)

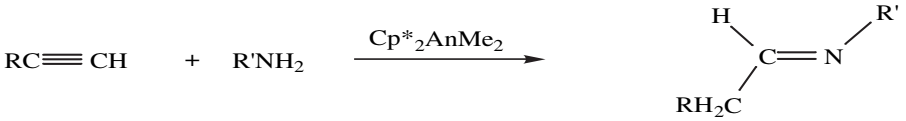

(2)

The metal-catalyzed hydrosilylation reaction, which is the addition of a Si-H bond across a carbon-carbon multiple bond, is one of the most important reactions in organosilicon chemistry and has been studied extensively for half a century. Considerable attention has been paid in recent years to the versatile and rich chemistry of vinylsilanes, which are considered as important building blocks in organic synthesis. The synthesis of vinylsilanes has been extensively studied, and one of the most convenient and straightforward methods is the hydrosilylation of alkynes. In general, hydrosilylation of terminal alkynes produces the three different isomers, *cis*, *trans* and *geminal*, as a result of both 1,2 (*syn* and *anti*) and 2,1 additions, respectively. The distribution of the products is found to vary considerably with the nature of the catalyst, substrates and also the specific reaction conditions. We have recently shown that organoactinides complexes of the type $Cp^*_2AnMe_2$ ($Cp^* = C_5Me_5$; An = U, Th) are active catalysts for the hydrosilylation of terminal alkynes with silanes of terminal alkynes, and the extent of oligomerization was found to be strongly dependent on the electronic and steric properties of the alkyne substituents.[4]

The room temperature reaction of $Cp^*_2AnMe_2$ (An = Th, U) with an excess of terminal alkynes RC≡CH and $PhSiH_3$ (alkyne:silane:catalyst = 40:40:1) in either benzene or tetrahydrofuran results in the catalytic formation of *trans*-vinylsilane

CP532, Plutonium Futures – The Science, edited by K. K. S. Pillay and K. C. Kim,

RCH=CHSiH$_2$Ph , the dehydrogenative silylalkyne RC≡CSiH$_2$Ph and the corresponding alkenes RCH=CH$_2$ as shown in equation 3.

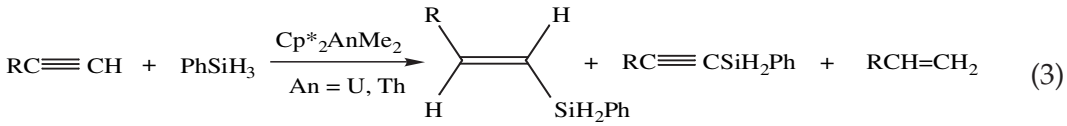

(3)

The corresponding hydrosilylation reactions using Cp*$_2$ThMe$_2$ with PhSiH$_3$ and the terminal alkynes RC≡CH (R = ^{t}Bu, ^{i}Pr, ^{n}Bu) (alkyne:silane:catalyst = 40:40:1), at high temperature follows the regioselectivity and chemoselectivity as obtained for the hydrosilylation reaction at room temperature (eq. 3). The only difference was found for isopropylacetylene; for it, no hydrogenated alkane was produced, and the double hydrosilylated product ^{i}PrCH=C(SiH$_2$Ph)$_2$ was achieved.

The stoichiometric and catalytic properties of organo-f-element complexes are deeply influenced by the nature of the p ancillary ligands. Structurally, a considerable opening of the metal coordination sphere (frontier orbitals) at the s-ligand equatorial girdle is obtained by replacing the pentamethylcyclopentadienyl ligation in Cp*$_2$MR$_2$ (Cp*= C$_5$Me$_5$, M = f-element metal, R = s-bonded ligand) by a bridged ligation towards the corresponding *ansa*-Me$_2$SiCp″$_2$MR$_2$ (Cp″ = C$_5$Me$_4$). We have shown above that organoactinides of the type Cp*$_2$MR$_2$ are active catalysts for either the oligomerization of terminal alkynes or the hydrosilylation of terminal alkynes with PhSiH$_3$. In the former catalytic process the reaction proceeds slowly with no regioselectivity for small alkyne substituents. The lack in regioselectivity is obtained because of the different mode of insertion of the terminal alkyne at the metal-carbyl bond, at each growing step. In the latter catalytic process—hydrosilylation—the reaction produces a myriad of hydrosilylated and hydrogenated products due to parallel competition processes. Thus, a conceptual question arises regarding the use of a more open organoactinide such as Me$_2$SiCp″$_2$Th^{n}Bu$_2$ as compared to Cp*$_2$MR$_2$. This opening in the coordination sphere at the metal center was shown to increase the reactivity and at the same time the *selectivity* of the products in both oligomerization and/hydrosilylation catalytic processes since any approach to the metal center through the equatorial plane is selectively hindered by the methyl groups of the bridged ancillary ligation. In this presentation we report, and quantitatively compare, the effects of the *ansa*-organothorium complex Me$_2$SiCp″$_2$Th^{n}Bu$_2$ for the chemo- and regio-selective dimerization of terminal alkynes as well as the extremely rapid regioselective hydrosilylation of terminal alkynes with PhSiH$_3$ as compared to the open organoactinides.[5] In every case the full characterization of compounds (x-ray), kinetics and thermodynamic data will be presented. Plausible mechanisms are proposed.

Refrences

1 T. Straub, A. Haskel A. K. Dash and M. S. Eisen *J. Am. Chem. Soc.* **121** (1999) 3014-3024.

2 A. Haskel, J. Q. Wang, T. Straub, T. Gueta-Neyroud and M. S. Eisen *J. Am. Chem. Soc.* **121** (1999) 3025-3034.

3 (a) T. Straub, W. Frank, G. J. Reiß, and M. S. Eisen. *J. Chem. Soc., Dalton Trans.* (1996) 2541-2546. (b) A. Haskel, T. Straub, M. S. Eisen *Organometallics* **15** (1996) 3773-3776.

4. A. K. Dash, J. Q. Wang and M. S. Eisen *Organometallics* **18** (1999) 4724-4741.

5. A. K. Dash and M. S. Eisen unpublished results.

A Novel Equation for Predicting Stability Constants of Aqueous Metal Complexes and Actinide Binding to Protein

Huifang Xu,
Department of Earth and Planetary Sciences, University of New Mexico, Albuquerque, NM 87131, USA

Yifeng Wang
Sandia National Laboratories, Carlsbad, NM 88220, USA

Metal complexation with various inorganic or organic ligands in aqueous solutions directly controls the solubility, sorption, and toxicity of toxic metals including radionuclides in natural environments. The quantitative calculations of metal complexation thus have been routinely used in predicting the fate and impact of heavy metals in natural environments. The effectiveness of these calculations heavily depends on the completeness and quality of the thermodynamic databases on which the calculations are based. Unfortunately, the thermodynamic data for many metal complexes, especially those with radionuclides, are currently either unknown or poorly constrained. Therefore, there is a need for (1) developing a method to predict the unknown thermodynamic data based on a limited number of the existing measurements and (2) using this method to check the internal consistency of the thermodynamic databases that are used in the calculations.

The stability constants (K_{ML}) for a family of metal complexes can be correlated to the non-solvation energies ($\Delta G^0_{n,M}n+$) and the radii ($r_M n+$) of cations by equation:

$$2.303RT\,log K_{ML} = -a^*_{ML}\,\Delta G^0_{n,M}n+ - b^{**}_{ML} - b^*_{ML}\,r_M n+ + \Delta G^0_{f,M}n+,$$

where the coefficients a^*_{ML}, b^{**}_{ML}, and β^*_{ML} characterize a particular family of metal complexes.

The equation can be used to predict the Gibbs free energies of formation or stability constants for a family of metal complexes and chelates with a given complexing ligand. The equation can also be used for predicting binding strength of metals and actinides to a protein of human serum transferrin (hTF) (Figure).

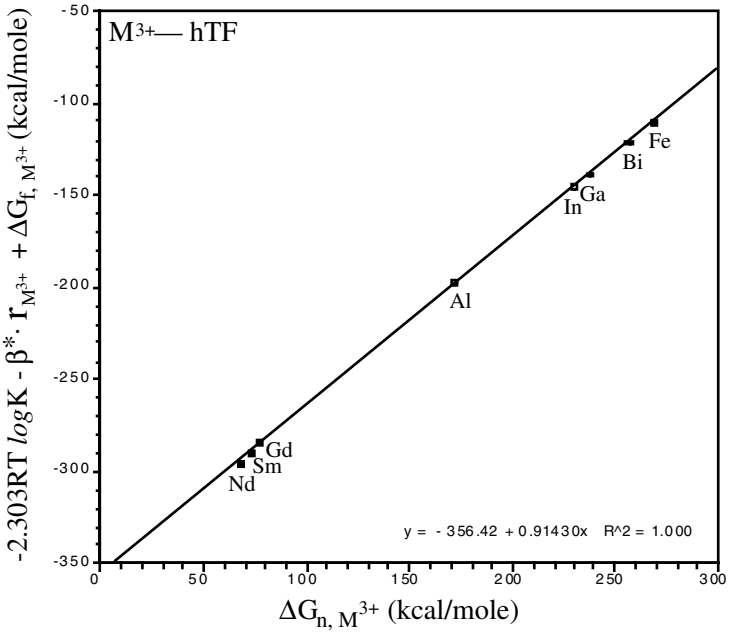

Figure 1. Linear free energy relationship of the equation for M3+-hTF (*log* K) complexes.

The linear free energy relationship is a function of non-solvation energy and inonic radii of cations. The relationship can be applied to both inorganic and organic metal complexs/ chelates. The discrepancies between the predicted and experimental data are generally less than one log unit. The use of this linear free energy correlation can significantly enhance our ability to predict the speciation, mobility, and toxicity of heavy metals and actinides in natural environments.

CP532, Plutonium Futures – The Science, edited by K. K. S. Pillay and K. C. Kim,
2000 American Institute of Physics 1-56396-948-3

Radiation Effects in Uranium-Niobium Titanates

J. Lian,
S. X. Wang,
L. M. Wang,
R. C. Ewing
University of Michigan, Ann Arbor, MI 48109-2104, USA

Pyrochlore is an important actinide host phase proposed for the immobilization of high level nuclear wastes and excess weapon plutonium.[1] Synthetic pyrochlore has a great variety of chemical compositions due to the possibility of extensive substitutions in the pyrochlore structure.[2] During the synthesis of pyrochlore, additional complex titanate phases may form in small quantities. The response of these phases to radiation damage must be evaluated because volume expansion of minor phases may cause micro-fracturing. In this work, two complex uranium-niobium titanates, $U_3NbO_{9.8}$ (U-rich titanate) and Nb_3UO_{10} (Nb-rich titanate) were synthesized by the alkoxide/nitrate route at 1300°C under an argon atmosphere. The phase composition and structure were analyzed by EDS, BSE, XRD, EMPA and TEM techniques. An 800 KeV Kr^{2+} irradiation was performed using the IVEM-Tandem Facility at Argonne National Laboratory in a temperature range from 30 K to 973 K. The radiation effects were observed by *in situ* TEM.

At room temperature, the critical amorphization doses (D_c) of U-rich titanate and Nb-rich titanate irradiated by 800 KeV Kr^{2+} are 4.72×10^{17} (0.10 dpa according to the TRIM-96 calculation) and 5×10^{17} ions/m^2 (0.11dpa), respectively. No significant difference of critical amorphization dose was observed between the U-rich and Nb-rich titanates. The temperature dependences of the critical amorphization doses are shown in Fig. 1. With increasing temperature, the critical amorphization doses increase as a result of dynamic annealing. The critical amorphization temperature for both Nb-rich and U-rich phases is ~ 933 K.

Above the critical amorphization temperature, full amorphization does not occur, and nanocrystal formation was observed. Fig. 2 shows the microstructure of the U-rich titanate irradiated at 933 K at an ion dose of 2.5×10^{19} ions/m^2. Nanocrystals have a preferred orientation, and the average size is 15 to 20 nm. The microstructure of U-rich titanate irradiated by 1.88×10^{19} ions/m^2 Kr^{2+} at 973 K is shown in Fig. 3. Nanocrystals with a random orientation were observed.

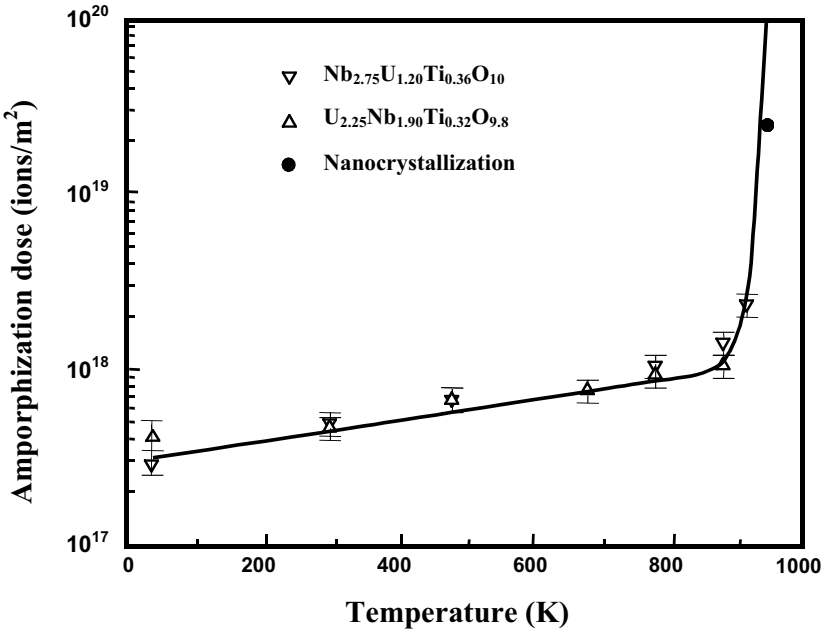

Figure 1. Temperature dependences of critical amorphization doses of the U-rich and Nb-rich titanates irradiated by 800 KeV Kr^{2+}. The black dot denotes the formation of nanocrystals at 933 K.

CP532, Plutonium Futures – The Science, edited by K. K. S. Pillay and K. C. Kim,

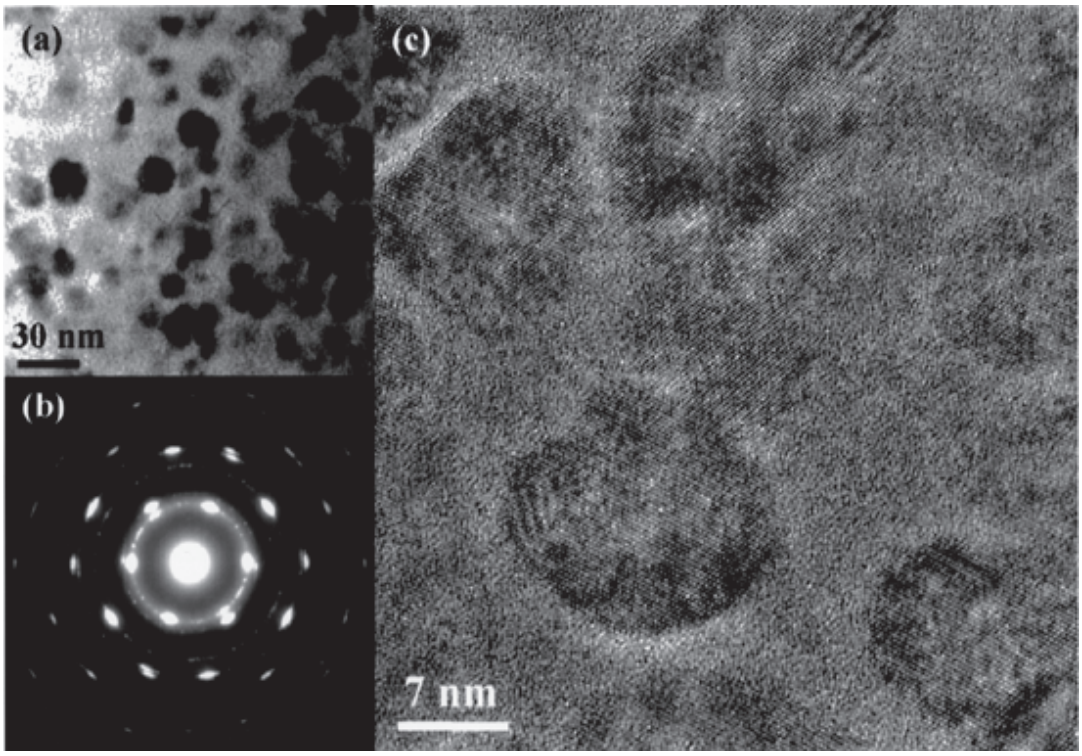

Figure 2. (a) Bright-field image; (b) SAD pattern; (c) HRTEM image of U-rich titanate irradiated by 800 KeV Kr^{2+} at 933 K.

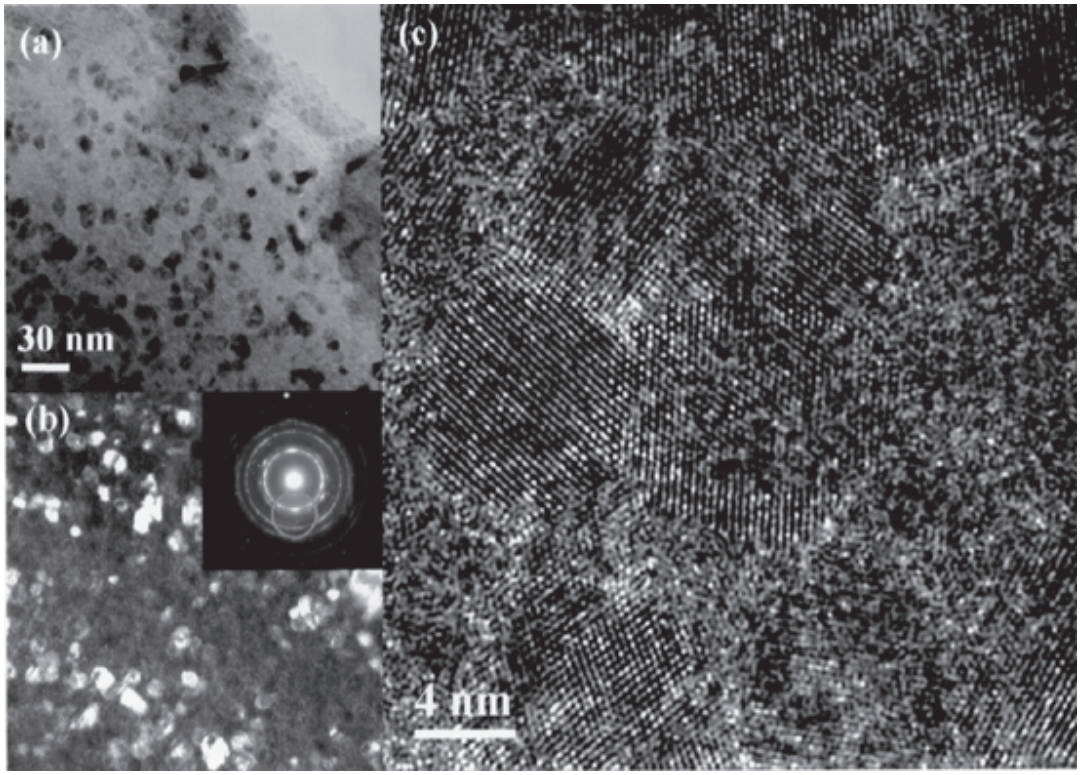

Figure 3. The microstructure of U-rich titanate irradiated by 800 KeV Kr^{2+} at 973 K with ion dose of 1.8×10^{19} ions/cm^2: (a) Bright-field image; (b) Dark-field image; (c) HRTEM image.

Ion irradiation-induced nanocrystal formation can be the result of competition between amorphization and crystal recovery and recrystallization.[3-5] Epitaxial growth and nucleation-growth are the primary crystal recovery mechanisms during the process of ion irradiation-induced amorphization. Due to the higher energy barrier for the formation of new crystal nuclei, the probability of nucleation-growth is small as compared with that of epitaxial growth. Thus, the epitaxial recrystallization of the highly damaged materials leads to the formation of nanocrystals at 933 K. As a result, nanocrystals show a preferred orientation similar to that of the original crystalline matrix. At a higher temperature, 973 K, the probability of nucleation increases due to the lower quench rate and longer annealing time. Thus, nanocrystals of random orientation can form around these newly formed nuclei. In this case, ion irradiation-induced nucleation-growth of nanocrystals that occurs in heavily damaged crystalline materials at elevated temperature is similar to thermally activated recrystallization in cold-worked metals.[6,7] Epitaxial growth and ion irradiation-induced nucleation-growth both have important effects on the formation and orientation of nanocrystals.

Acknowledgement

We thank Dr. L. Vance at Australia Nuclear Science and Technology Organization for preparing the samples used in this study.

References

1. R. C. Ewing, W. J. Weber, W. Lutze, in: E. R. Merz, C. E. Walter (Eds.), Disposal of Weapon Plutonium, Kluwer Academic Publishers, Boston, MA, 1996, 65.

2. B. C. Chakoumakos, R. C. Ewing, Mat. Res. Soc. Symp. **44** (1985) 641

3. L. M. Wang, et al., submitted to Mater. Sci. and Engin. A, 1999.

4. A. Meldrum, et al., Canadian Mineralogist **37** (1999) 207.

5. A. Meldrum, S. J. Zinkle, L. A. Boatner, R. C. Ewing, Nature **395**, 3 (1998) 56.

6. L. M. Wang, R. C. Birtcher, R. C. Ewing, Nucl. Instr. and Meth. B **80/81** (1993) 1109.

7. R. C. Birtcher, L. M. Wang, Nucl. Instr. and Meth. B **59** (1991) 966.

Electronic and Geometric Structure of Pu Metal: A High-Resolution Photoelectron Spectromicroscopy Study

J. Terry,
R. K. Schulze,
T. Zocco,
Jason Lashley,
J. D. Farr
Los Alamos National Laboratory, Los Alamos, NM 87545, USA

K. Heinzelman,
E. Rotenberg,
D. K. Shuh
Advanced Light Source, Lawrence Berkeley National Laboratory, Berkeley, CA 94720, USA

M. Blau,
J. Tobin
Lawrence Livermore National Laboratory, Livermore, CA 94550, USA

Introduction

The physical characteristics of any given material are largely derived from the behavior of its valence electrons. Valence electrons are the lowest energy electrons in a material and are responsible for the formation of chemical bonds. Typically, in a metal, electrons are either localized around a particular atom or are delocalized (i.e., shared by all the atoms in the crystal) throughout the entire metal. The actinide series is interesting because as the atomic number increases across the series, the electrons in the actinide metals make a transition from delocalized 5f electrons (Ac–Pu) to localized 5f electrons (Pu–No). Plutonium (element 94) is located right at this transition. This placement in the series leads to plutonium metal being one of the most complex materials known. Metallic plutonium displays six allotropic phases (α, β, γ, δ, δ′and ε) at standard pressure. A 20% volume expansion occurs during the change from the a phase to the δ phase. These physical properties have been attributed to the 5f valence electrons changing from delocalized states to localized states as the crystal structure changes from the α phase to the δ phase.

Soft x-ray techniques (photon energy in the range of 10–1000 eV) such as photoelectron; x-ray emission; and near-edge, x-ray absorption spectroscopies have been used to determine the electronic structure of many (in fact most) materials. However, these techniques have not been fully utilized on the actinides. The safety issues involved in handling the actinides make it necessary to minimize the amount of radioactive materials used in the measurements. To our knowledge, the only synchrotron radiation source in the world where soft x-ray measurements have been performed on plutonium is the Spectromicroscopy Facility at Beam Line 7.0.1 at the Advanced Light Source (ALS).

The Spectromicroscopy Facility is designed so that measurements can be made on small quantities of hazardous material. This facility has a photon flux of 10^{13} photon/sec at a photon energy of 100 eV with 0.01 eV resolution. The high photon flux allows one to focus the beam down to a size of 50 microns and still have enough light intensity at the sample for measurements to be conducted in a reasonable time frame 1–10 minutes per spectrum. Therefore, the sample size can be on the order of 100 microns in diameter. This greatly minimizes the amount of plutonium on site during the experiment.

Results

We performed core-level photoemission, valence band photoemission, and near-edge x-ray absorption spectroscopy on both polycrystalline α-plutonium and δ-plutonium microcrystals. Only the photoemission experiments will be described here. Photoelectron spectroscopy is predicated upon the photoelectric effect first described by Einstein in 1905. An incident photon is absorbed by an atom in the solid, and an electron is ejected. An electron energy analyzer is used to measure the direction and kinetic energy of the emitted electron. The kinetic energy of the photoelectron is directly related to its binding energy in the solid.

CP532, Plutonium Futures – The Science, edited by K. K. S. Pillay and K. C. Kim,
2000 American Institute of Physics 1-56396-948-3

Figure 1 shows the Pu 4f core-level photoemission spectra from the α- and δ-plutonium samples. The spectrum arising from core-level photoemission is sensitive to energy differences in the initial state (no core hole) and the final state (core hole and free photoelectron). The two core-level spectra in Figure 1 are similar in that they both show two features, a sharp feature at low binding energy and a broad feature at higher binding energy. The low-binding-energy feature can be ascribed to a metallic initial state with a delocalized final state. As the 5f electrons are more delocalized in the α- than in the δ-plutonium; the greater number of delocalized electrons in the a-plutonium leads to greater intensity in this peak than the d-plutonium.

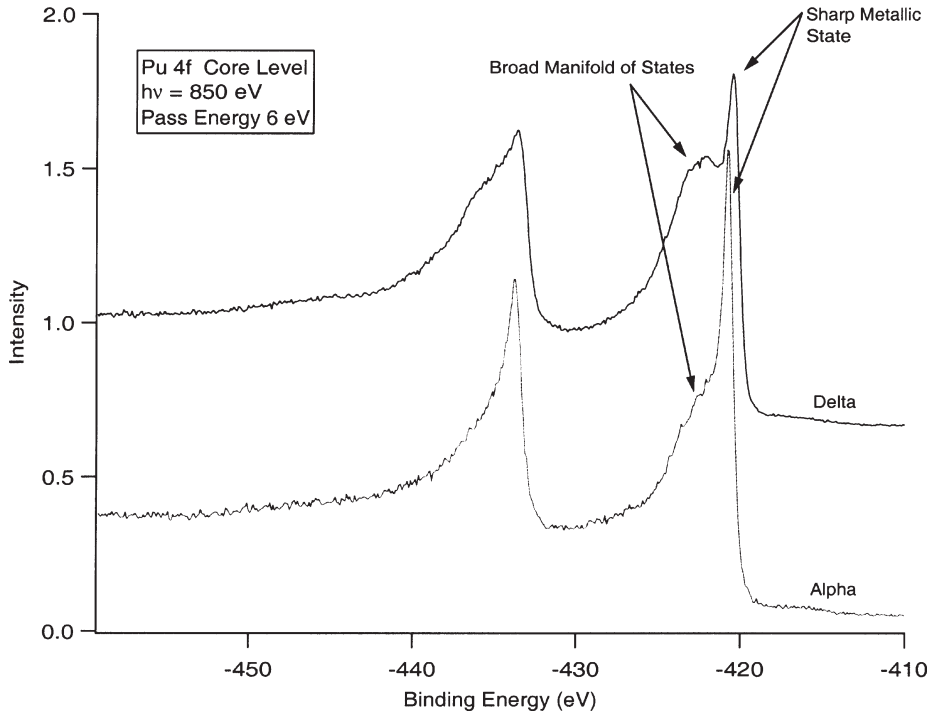

Figure 1. Core-level photoemission spectra from a large crystallite δ-plutonium sample and a polycrystalline α-plutonium sample are shown. These spectra were collected with a photon energy of 850 eV and an analyzer pass energy of 6 eV. Note that two large components are visible in each spectrum, a sharp feature at low binding energy and a broad feature at higher binding energy.

Presently, the higher-binding-energy feature is not completely understood. It is likely that this feature has two states contributing to it. We believe that, in simplistic forms, one possible component contributing to the feature is made up of emission to an electronic final state with localized 5f electrons. If this is the case, it suggests that both localized and delocalized 5f electrons are present in the a- and d-plutonium phases. The second possible component of this feature is from an initial state that has been oxidized.

Valence band spectra show that a small amount of oxygen remains on the surface after the sample preparation. The binding energy of PuO_x is higher than that of the metal and would be expected to be seen around the position of the unknown high-binding-energy feature. A final determination of the exact nature of this high-binding-energy feature will shed light on the poorly understood valence electronic structure of plutonium, as well as on the presence of localized and delocalized 5f electrons in the different plutonium phases.

Our initial goal of the valence electronic structure measurements was to determine the density-of-states of the 5f valence electrons in α- and δ-plutonium. This experi-

ment can be directly compared with electronic structure calculations performed by theoreticians. Figures 2(a and b) show the resonant photoemission spectra of the valence band from δ- and α-plutonium, respectively. In a resonant photoemission experiment, valence band photoemission spectra are collected as the photon energy is scanned through a core-level absorption edge. This can result in an enhancement of the emission from specific valence levels. In the case of plutonium, scanning the photon energy through the 5d absorption edge results in a resonant enhancement of the 5f valence emission. The 5d–5f resonant photoemission measurements in plutonium are a measurement of the 5f contribution to the valence density of states.

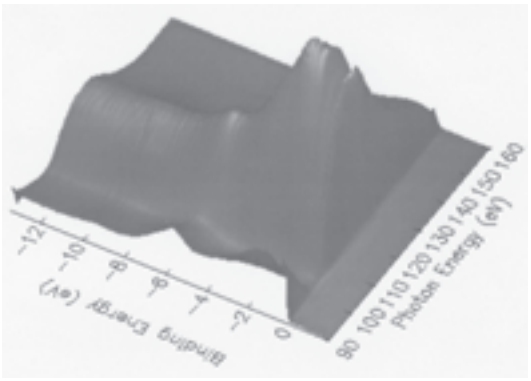

Figure 2(a). The 5d–5f resonant photoemission spectrum with analyzer pass energy of 1 eV showing the 5f density of states in the valence band from a large crystallite δ-plutonium sample.

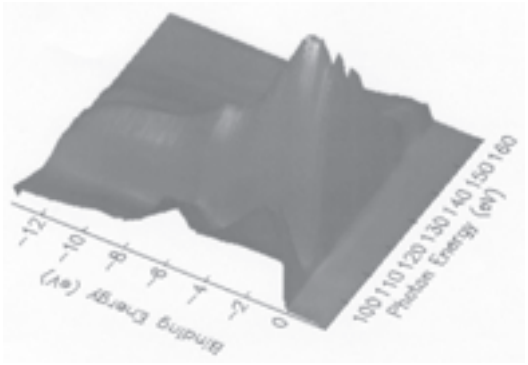

Figure 2(b). The 5d–5f resonant photoemission spectrum with analyzer pass energy of 1 eV showing the 5f density of states in the valence band from a polycrystalline α-plutonium sample.

Two types of information are obtained in the resonant photoemission measurements that can greatly enhance the understanding of plutonium metal. Two-dimensional data slices can be taken in either the constant-photon-energy direction or the constant-binding-energy direction. Slices taken with a constant photon energy are the equivalent to standard photoemission spectra with the exception that specific valence states are emphasized. Different states turn on or become enhanced at different photon energies.

The data in Figures 2(a and b) show clear differences in the resonant photoemission spectra from the α- and δ-plutonium. This is most evident in the state at binding energy 0 eV. If this peak is followed as the photon energy is varied, one notices that in the δ-plutonium (Figure 2a) after 100 eV, the peak smoothly increased to a maximum and then smoothly decreased after the maximum was reached. In direct contrast, the α-plutonium (Figure 2b) showed oscillatory behavior after the initial maximum was reached. Theoretical calculations of the resonant photoemission are currently ongoing to try to understand these differences.

A large theoretical effort has been undertaken to understand the plutonium data that we have collected. The next phase of the valence-band, electronic structure measurements will involve measuring the electron dispersion relation (band structure) of the valence electrons in δ-plutonium, and the data will be compared with theoretical calculations. The band structure can only be measured on a single crystal of a material, and it is imperative to have excellent crystals for the measurement. Future investigations will be based upon spin-resolving and photon-dichroic photoelectron spectroscopy. The photon-dichroic measurements include the variant magnetic x-ray linear dichroism.

The unique 5f valence electronic properties of plutonium metal cannot be explained by the typical one-electron calculations used to describe prototypical metals. Calculations on plutonium metal incorporate these properties into calculations in an ad hoc manner. We can measure these effects directly to further our understanding of one of the most complex materials known.

Acknowledgments

This is Los Alamos report number LAUR-99-1517. Los Alamos National Laboratory is is operated by the University of California under Contract No. W-7405-ENG-36. The Advanced Light Source is supported by the Director, Office of Energy Research, Office of Basic Energy Sciences, Materials Sciences Division, of the U.S. Department of Energy under Contract No. DE-AC03-76SF00098 at Lawrence Berkeley National Laboratory.

Preliminary Study of ($Pu_{1-x}Am_x$) Solid Solutions

F. Wastin,
E. Gomez-Marin,
D. Bouëxière,
J. C. Spirlet
European Commission, Joint Research Centre, Institute for Transuranium Elements, D-76125 Karlsruhe, Germany
J. M. Fournier
Université Joseph Fourier, Laboratoire LIME, 38041 Grenoble Cedex, France

Introduction

Among the actinides, plutonium is at the critical position between the light actinides with itinerant 5f electrons and the heavy actinides with localized 5f electrons. The change of behavior of the 5f electrons between Pu and Am has been described by Johansson[1] as a Mott-like transition. Although α-plutonium is monoclinic, and α-americium is hexagonal, plutonium alloys with Am exist over a wide range of solubility.[2] Am stabilizes the δ-Pu fcc structure in which 5f electrons are more localised. This localisation was attributed to a negative chemical pressure due to Am substitution in the Pu-lattice.[3] Therefore the $Pu_{1-x}Am_x$ solid solutions appear to be the ideal material to investigate the localisation phenomena of 5f electrons. In the present work, $Pu_{1-x}Am_x$ samples with various concentrations of Am were prepared by arc melting pure metals and studied by means of electrical resistivity measurements at low and high temperatures.

Experimental

$Pu_{1-x}Am_x$, with x = 0.06, 0.08, 0.1, 0.15, 0.20, 0.25, 0.30 and 0.45 were prepared by arc melting pure metals in stoichiometric amounts and turned over several times to ensure their homogeneity. Samples were then either "splat cooled" to get foils of about 400 mm thickness and 8 mm diameter or cast in copper molds to get rods of 2x2 mm and several cm length.

The samples obtained were characterised by X-ray diffraction, metallography and microprobe analysis. Homogeneity of Am distribution was checked by autoradiography. Electrical resistivity was measured at low (down to 1.5 K) and high temperatures (up to 800 K) on bulk samples (foils or rods) by a standard 4-point AC Lock-In technique in experimental setups adapted for measuring highly radioactive samples as described previously.[4,5]

Results and Discussion

Solid solutions were found to crystallize in the fcc cubic phase isostructural with δ-Pu and β-Am. At the present stage, resistivity measurements are only available for samples with x = 0.1, 0.25, 0.30 and 0.45. Resistivity curves obtained over the whole range of temperature are shown in Figure 1.

At low temperature (up to 20 K to 40 K, respectively, for high and low Am content) the resistivity follows a ρ_0+AT^2 type law suggesting a dominant contribution of interband diffusion phenomena. The variation of the A parameter with Am concentration, almost constant from $Pu_{0.5}Am_{0.5}$ to $Pu_{0.75}Am_{0.25}$, shows a strong increase for $Pu_{0.9}Am_{0.1}$ indicating considerable contribution of spin fluctuations. This suggests an enhancement of Pu magnetic moment coupling due to an increase of the 5f electrons' localisation. However, these results should be treated with care due to the large uncertainty in the determination of the absolute value of the resistivity.

CP532, Plutonium Futures – The Science, edited by K. K. S. Pillay and K. C. Kim,

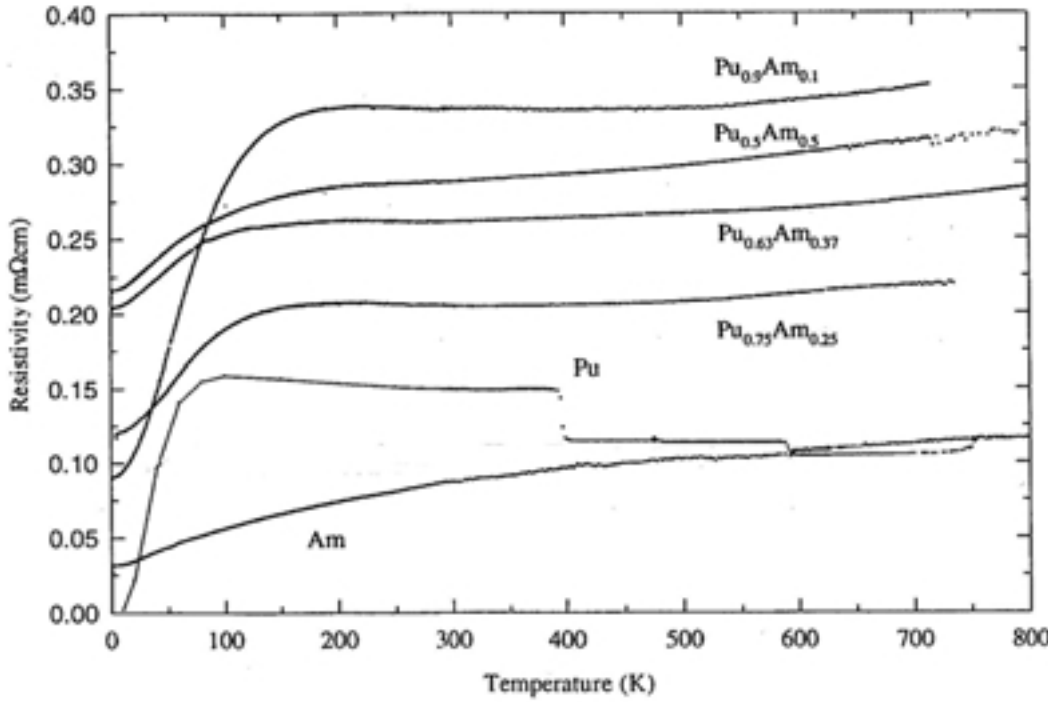

Figure 1. Temperature dependence of the resistivity of Pu-Am alloys.

At high temperature, the magnetic contribution of the alloys shows a Kondo type behavior (ρ ~a-b.lnT with b/a proportional to the integral exchange J between conduction electron and Pu moments[6]). It is observed that a and b slowly decrease as Am content increases, related to a decrease of the magnetic impurities (Pu) concentration whereas the variation of the b/a ratio shows a more complex variation. This is understood as being due to a decrease of the magnetic contribution with increasing Am content. Once a sufficient amount of Pu is substituted by Am to reach a critical increase of the Pu-Pu interdistances, the systems tend to a classical Kondo lattice behaviour of isolated magnetic impurities. These preliminary results are in good agreements with previous analysis of Pu alloys stabilised in the δ phase by Al,[7,8] Ga[8] or Ce,[8] but in order to shed more light on this localisation-delocalistion phenomena, further investigations by other techniques are required.

References

1. B. Johansson, Phil. Mag. 30 (1974), 469.
2. F. H. Ellinger, K. A. Johnson and V. O. Struebing, J. Nucl. Mater. 20 (1966), 83.
3. J. M. Fournier, Physica B 190 (1993), 50.
4. F. Wastin, PhD Thesis, University of Liège (1991).
5. E. Gomez-Marin, PhD Thesis, University of Grenoble (1997).
6. See e.g. J. M. Fournier and R. Troc in A. J. Freeman and G. H. Lander (eds), Handbook on the Physics and Chemistry of the Actinides, Vol.2, North-Holland, Amsterdam, 1985, Chapter.2, and references therein.
7. Y. A. Rocher, J. Friedel, J. Phys. Chem. Solids 18 2/3 (1961), 196.
8. S. Méot-Reymond and J. M. Fournier, J. Alloys and Compounds 232 (1996), 119.

Actinide Electronic Structure and Atomic Forces

R. C. Albers,
Sven P. Rudin,
Dallas R. Trinkle
Los Alamos National Laboratory, Los Alamos, NM 87545, USA

M. D. Jones
SUNY, Buffalo, NY 14260, USA

In order to develop a predictive capability of materials properties it is necessary to accurately determine the forces between the atoms in a solid. Most of the established molecular dynamics simulations involve either pair potentials, embedded-atom potentials, or, for covalent materials like Si, some classical potentials with additional bond-angle information. Unfortunately, these methods have proved inadequate for complex *d*-electron (transition-metal) and *f*-electron (actinide) systems, which have important bond-bending forces that seem difficult to capture in any simple way. The most promising approach for such systems is tight-binding (TB), which automatically builds in the quantum-mechanical bonding that conventional first-principles local-density approximation (LDA) or gradient corrected (GGA) band-structure calculations can very accurately determine.

We have developed a new method[1] of fitting tight-binding parameterizations based on functional forms developed at the Naval Research Laboratory.[2] We have applied these methods to actinide metals and report our success using them (see below). The fitting procedure uses first-principles local-density-approximation (LDA) linear augmented plane-wave (LAPW) band structure techniques[3] to first calculate an electronic-structure band structure and total energy for fcc, bcc, and simple cubic crystal structures for the actinide of interest. The tight-binding parameterization is then chosen to fit the detailed energy eigenvalues of the bands along symmetry directions, and the symmetry of the parameterization is constrained to agree with the correct symmetry of the LDA band structure at each eigenvalue and k-vector that is fit to. By fitting to a range of different volumes and the three different crystal structures, we find that the resulting parameterization is robust and appears to accurately calculate other crystal structures and properties of interest.

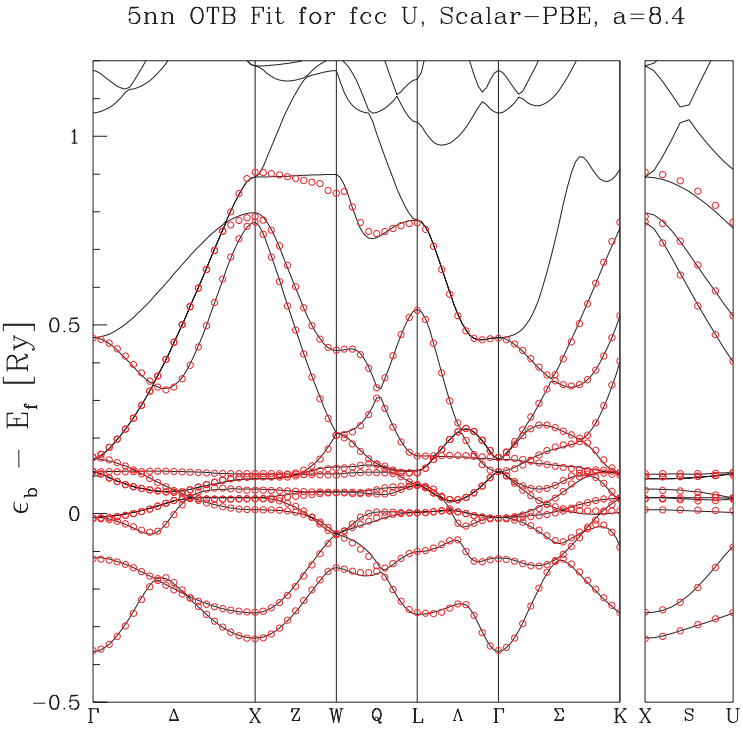

Figure 1. Comparison of tight-binding and LDA bands for U.

CP532, Plutonium Futures – The Science, edited by K. K. S. Pillay and K. C. Kim,
2000 American Institute of Physics 1-56396-948-3

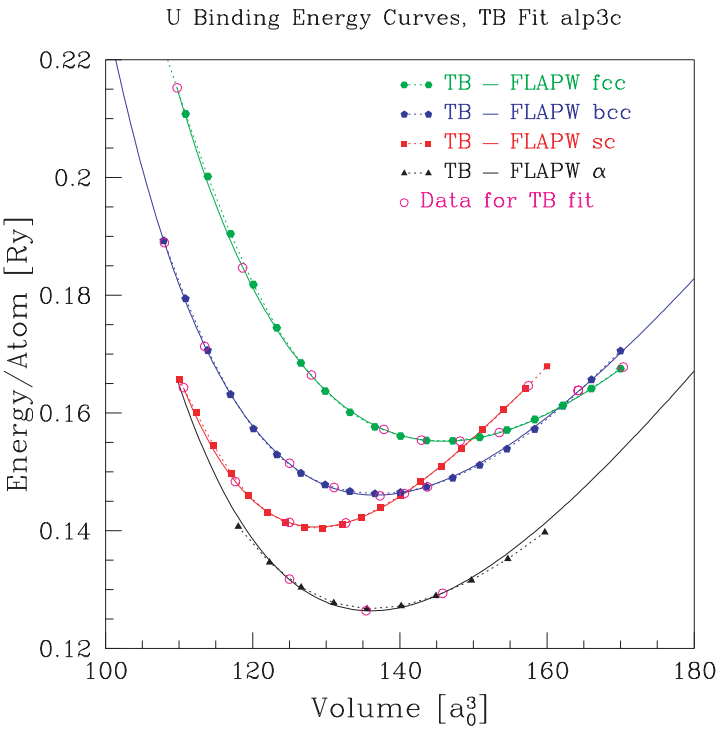

Figure 2. Energy vs. volume comparison between tight-binding and LDA for U.

In Fig. 1 we show a sample fit to a band-structure for uranium. As shown, we are able to obtain almost exact agreement between the fitted and first-principles band structures. In Fig. 2 we show the comparison between the total energies of the LDA calculations and our tight-binding fits. Again, agreement is virtually exact, even for the very asymmetric a-phase. We have also been successful in calculating the charge-density-wave (CDW) in a-U using the tight-binding fits.

References

1. M. D. Jones and R. C. Albers, unpublished.

2. R. E. Cohen, M. J. Mehl, and D. A. Papaconstantopoulos, Phys. Rev. B **50**, 14964 (1994). M. J. Mehl and D. A. Papaconstantopoulos, Phys. Rev. B **54**, 4519 (1996). S. H. Yang, M. J. Mehl, and D. A. Papaconstantopoulos, Phys. Rev. B **57**, R2013 (1998).

3. D. J. Singh, *Planewaves, Pseudopotentials and the LAPW Method*, (Kluwer, Boston, 1994).

Determination of Mechanical Properties of Aged Plutonium from ARIES Pits by Instrumented Sharp Indentation

Tonya Huntley, Kaye Johnson, David Olivas, Robi Mulford, Wendel Brown, Kevin Walter, Mike Stout
Los Alamos National Laboratory, Los Alamos, NM 87545, USA

Introduction

We are studying the effects of extended aging in very old weapons-grade plutonium that is being recovered from pits being destroyed for material disposition (MD) purposes. This study is a piggyback study to the demonstration of the Advanced Recovery Integrated Extraction System (ARIES). The plutonium in the weapons selected for ARIES has a unique combination of advanced age and varied service history.

The major goal of this study is to determine mechanical properties of aged pit materials. Long-term, safe storage of plutonium from pits depends upon several properties, including the strength and dimensional stability of the metal. A large amount of concrete data about the structure and mechanical properties of plutonium has been accumulated over many years, but very little of this data has a bearing on the properties of the metal as it ages.

Description of Actual Work

We selected instrumented sharp indentation as the means to determine the mechanical properties of plutonium extracted from ARIES pits. This form of micro-indentation allows us to use a plutonium sample about the size of a U.S. quarter dollar and still permits space on the sample for other tests such as metallography and x-ray diffraction.

Our work is based on recent papers written by Dr. Subra Suresh of M.I.T. Using Dr. Suresh's theory, we have extracted the yield strength, ultimate tensile strength, and Young's Modulus, and expect to extract the strain hardening coefficient and residual stresses. Residual stresses in weapons are more than likely a result of the various methods used to manufacture the pits and the various service histories of the pits (e.g., different storage temperatures).

We use a hydraulic punch driver to obtain samples approximately the size of a U.S. quarter dollar from the ARIES pits. By obtaining samples using a punch driver, we are able to avoid excess sample preparation and preserve the inner region of the punched samples for study without deformation or work hardening.

To perform the instrumented sharp indentation on the samples, we purchased two Micro Photonics Inc. micro-indentation test systems (Model MHT). One will be placed inside a glovebox for testing plutonium, and the other will remain cold. These modern indentation machines are quite different from the older styles, which required measuring indentation diagonals optically. The modern machines take continuous readings of the applied load versus the depth of penetration during the indentation as the load is both applied and removed. Since more than ten indents can be taken on a sample in less than 15 minutes, good statistical confidence can be readily achieved.

CP532, Plutonium Futures – The Science, edited by K. K. S. Pillay and K. C. Kim,
2000 American Institute of Physics 1-56396-948-3

During each indentation test, a number of parameters can be controlled. These include loading and unloading rates, maximum load, and maximum indentation depth. For soft materials, we apply a maximum load of 10,000 mN (~1 kg) at a rate of 10,000 mN/min and then unload at a rate of 50,000 mN/min. The maximum load is sufficient to create a measurable indent, while the unloading rate is fast enough to minimize creep.

Results

We have performed hundreds of instrumented sharp indentation tests on Aluminum-1100 (Al-1100) and will perform tests on plutonium metal once the indentation machine is made operational in the glovebox. Al-1100's yield and ultimate tensile strengths are close to those of delta-phase plutonium. We have also conducting indentation tests with copper and stainless steel.

Our intent is to compare the mechanical properties derived from indentation tests to the results from well-known conventional mechanical tests (tensile and compressive) on similar samples. This will provide us with understanding regarding both the precision and the accuracy of the indentation testing technique.

We have performed indentation tests on rough and polished surface Al-1100, oxygen-free copper, and 304 stainless steel. The ultimate tensile strength results are shown below. The theory for determining yield strength is less well developed.

	Indentation	**Compression[1]**
Material	σ_{UTS} (MPa)	σ_{UTS} (MPa)
Aluminum 1100 (Polished Surface)	**100**	**105-110**
Aluminum 1100 (Rough Surface)	**100**	**105-110**
Oxygen-free Copper (99.95 % Cu)	**418**	**260**
304 Stainless Steel	**658**	**>600**

[1]The materials were tested at room temperature, under compression at a rate of 10^{-3}/sec.

Another goal of our study is to determine mechanical properties for different phases of inhomogeneous plutonium. We have performed indentation tests on

plutonium-simulate material (a Ce-5La alloy developed by Dr. Frank Gibbs) in two conditions: homogenized and partially homogenized. By comparing the two, we will observe possible differences in mechanical properties.

In plutonium, any aging effects brought about by varying temperatures and pressures while in service may affect the mechanical integrity of the metal. So, having some indication of the presence of more than one phase or other effects in the plutonium may help define the appropriate service environments.

Density of Plutonium Metal as a Function of Age

R. N. Mulford,
M. Valdez
Los Alamos National Laboratory, Los Alamos, NM 87545, USA

Densities of a large number of samples old plutonium metal are being measured, to determine the magnitude of density changes as a function of metal age. Radioactive decay produces helium within the metal lattice structure. Simultaneously, radioactive decay disrupts the metal lattice, producing dislocations and vacancies, which may or may not be occupied by the helium produced. The net effect of the conjunction of these effects is a decrease in the bulk density of the metal with time. This phenomenon has been seen in other metals,[1] and exhibits an induction time which depends on the metal and on the rate of helium ingrowth.

The immediate purpose of the measurements is to determine the induction time for Pu metal, and the magnitude of the density change to be expected in the metal with age. The functional form of these trends may, by analogy with other metals,[1,2] illuminate the phenomena described above.

These data complement other measurements, such as x-ray diffraction determination of lattice constants, which measure absolute lattice expansion with time, and direct measurements of helium content in the metal. The total helium content in a sample can be measured as a destructive test, after completion of density and other measurements. The amount of helium can alternatively be estimated quite accurately from the known radioactive decay rate and age of the metal, and a measurement of net helium evolved at the surface of the metal over time.

The plutonium metal is obtained from sources aged under known, controlled conditions for periods of up to 32 years. The method of metal preparation, while not recorded in detail, is known to have been uniform over large groups of samples. When small samples are required, cutting is done in such a way as to minimize distortion of the metal, and to minimize damage at sample edges.

Densities are measured using a precision immersion balance apparatus. The precision is 0.01 g/cc for samples of this type. The precision is augmented by care in selection of the immersion fluid, and by careful modification of the technique to take into account heating of the immersion fluid by the self-heating of the plutonium sample. Times of up to an hour are required for thermal stabilization of the immersion fluid around the plutonium metal sample. Frequent calibration against invar metal samples and against a set of National Bureau of Standards (NBS) calibrated samples provide a check on the accuracy of the measurements and of the stability of the system over time.

Data analysis uses statistical methods to take advantage of the relatively large number of samples, 60 to 80, to overcome both limitations in precision of the technique, and sample-to sample variation. Not only average values, but confidence tolerance bounds can be determined, giving an accurate estimate of the magnitude of variation within the sample population.

Dislocation density increases with the time of irradiation.[1] However, under the relatively high energy of the plutonium decay (5 MeV for the α, 85keV for the recoil U atom), thermal annealing follows the damage cascade, removing most of the decay-generated dislocations.[3]

CP532, Plutonium Futures – The Science, edited by K. K. S. Pillay and K. C. Kim,
2000 American Institute of Physics 1-56396-948-3

The induction time for onset of volume expansion in metals depends on vacancy and dislocation formation up to a critical defect population, but also on helium mobility, as helium moving into a newly formed vacancy may stabilize the structure. Helium occupation may increase or decrease the energy associated with dislocations. However, because helium results in stiffening of the lattice, the helium ingrowth locks dislocations. To the extent that helium mobility can be estimated from theory and from measured helium evolution at the metal surface, measurement of the induction time for density change in plutonium may directly indicate population density of voids and possibly dislocations generated during radioactive decay.

Density of both dislocations and stabilized voids have implications for mechanical properties and ultimately for physical integrity of the metal.[1,4] Measurement of the induction time for volume expansion, besides providing useful indications of time scales for material performance, may provide some of the time constants for dislocation formation and annihilation, void migration, and helium migration.

References

1. J. R. Weir, "The Effect of High Temperature Reactor Irradiation on Some Physical and Mechanical Properties of Beryllium," in *The Metallurgy of Beryllium*, Institute of Metals, London, 1963.

2. J. B. Adams and W. G. Wolfer, J. Nucl. Matls., **166**, p. 235 (1989).

3. V. G. Kapinos and D. J. Bacon, Phys. Rev. B, **50**(18), pp. 13194-203 (1994).

4. D. K. Tappin, D. J. Bacon, C. A. English, and W. J. Phythian, J. Nucl. Matls., **205**, pp. 92-7, (1993).

Electronic Structure of Elements and Compounds and Electronic Phases of Solids

B. A. Nadykto
RFNC-VNIIEF, Arzamas-16 (Sarov), Nizhni Novgorod Region, 607190, Russia

The paper reviews technique [1] and computed energies for various electronic states of many-electron multiply charged ions, molecular ions, and electronic phases of solids. The model used allows computation of the state energy for free many-electron multiply charged ions with relative accuracy ~10^{-4} suitable for analysis of spectroscopy data.

Energies of many-electron atoms and ions can be evaluated from solution to the Schroedinger equation using the variational method with trial wave functions as a simple product of hydrogen-like wave functions for each electron (with its own parameter) and relevant model potential.

The $1s^2 2s^2 2p^N$ state energy is described under the assumption of hybrid state formation for all N + 2 electrons. All of these electrons are characterized with an identical wave function parameter. Energy of the following electron shells can be calculated similarly. It is possible to find proper energy values for the ground state of ions with different nucleus charge Z. Having described the ground state energy, energies of numerous one-electron excited states of ions with the number of electrons higher by one can be calculated.

It is shown that energies of excited electron states of molecules can be calculated reasoning from classification of similar atomic states. For the hydrogen molecule the energy of excited states of the outer electron in the nuclei field and the inner electron is described well with this approximation.

The paper presents a model for compressed atom energy computation and derivation of the semi-empirical equation of state of solids using it. The model was used as a basis to obtain analytical expressions for dependencies of elastic energy and elastic pressure on the degree of compression describing the experiment well for many materials. The method used allows relating the energy variation at material compression with equilibrium energy of outer electrons in the solid atomic cell and estimating this effective energy from solid compressibility data.

Electronic phases of solids are discussed. Energy values are presented for outer electrons of the elementary atomic cell for many solid compounds obtained from computational analysis of experimental compressibility data [2]. The data refer both to compounds in the equilibrium state at standard pressure and temperature and to various phases of the solids appearing under high pressure in static or shock-wave experiments. Parameters are estimated, and the equation of state of each material phase is calculated. Under pressure new electronic phases are observed with equilibrium density both higher and lower than the initial phase density. The solid elementary atomic cell outer electron energy can differ very considerably for different phases (for example, by a factor of about 80 in different cesium phases).

The multiple solid electronic phases reflect the variety of energies of electron excited states observed in spectroscopy. The difference is that in spectroscopy energy levels of free atoms and molecules are observed, whereas in solid phases those of the fixed-volume atom are.

CP532, Plutonium Futures – The Science, edited by K. K. S. Pillay and K. C. Kim,

State energies of outer valent s, p, d electrons for lanthanide and actinide elements are compared. For one-electron excited states f electrons can be considered essentially always as Rydberg ones having energy $E= - 1/2n^2$. In actinides 5f electrons can hardly be considered as valent electrons in compounds and solids because of very low bond energy (0.54 eV for a single outer 5f electron).

References

1. Nadykto B. A., // UFN. 1993. V. 163, No. 9. Pp. 37-75.

2. Nadykto B .A., // VANT. Ser. Teor. i Prikl. Fizika. 1996. No. 3. p. 58-73.

5f Band Dispersion in the Highly Correlated Electronic Structure of Uranium Compounds

D. P. Moore,
J. J. Joyce,
A. J. Arko,
L. Morales,
J. Sarrao
Los Alamos National Laboratory, Los Alamos, NM 87544, USA

Despite the fact that the 5f shell of the light actinides is less than half filled, the relatively short radial extent of 5f-electron wave functions yields at most minimal f-f overlap (*the critical actinide-actinide spacing for which f-f overlap is no longer viable was first quantified by H. Hill and found to be 3.4 Å. The spacing for both USb_2 and UAsSe is about 4.5. Å*) and results in a myriad of phenomena collectively called correlated electron behavior. Ordered magnetism as well as heavy fermion phenomena are prevalent. For these two cases it is generally believed that the f-electrons are nearly localized, and it is the delicate interplay between the small residual hybridization with the valence bands and Coulomb exchange which determines whether a material favors the magnetic or the heavy fermion state. Band behavior of f-electrons has not been considered likely for An-An spacings greater than the Hill criterion.

The Anderson Impurity Hamiltonian is most often used as the starting point in theoretically describing uranium compounds (spacing greater than the Hill criterion) with its three 5f electrons although it has been recognized that this model presents problems for 5f systems. Within this model it is assumed that the 5f electrons behave as localized non-interacting magnetic impurities at high temperatures. Upon lowering the temperature one either obtains a magnetic state (exchange predominates) or a heavy fermion singlet state (hybridization predominates). In neither case does one expect band behavior of f-electrons. In Figs. 1 and 2 we present angle resolved photoemission data for antiferromagnetic USb_2 and ferromagnetic UAsSe respectively, both of which far exceed the Hill criterion and in which the 5f electrons are expected to be purely localized, especially when taking the magnetism into consideration. Instead we find that the 5f′ electrons clearly display band behavior and are strongly hybridized with the 6d electrons. In each figure the 40 eV photon energy data is about equally sensitive to 5f and 6d bands, while the 60 eV photon energy data represents primarily 5f emission. In both materials the 5f bands are peaked near the center of the zone, and then appear to disperse downward from the Fermi energy, and never cross it.

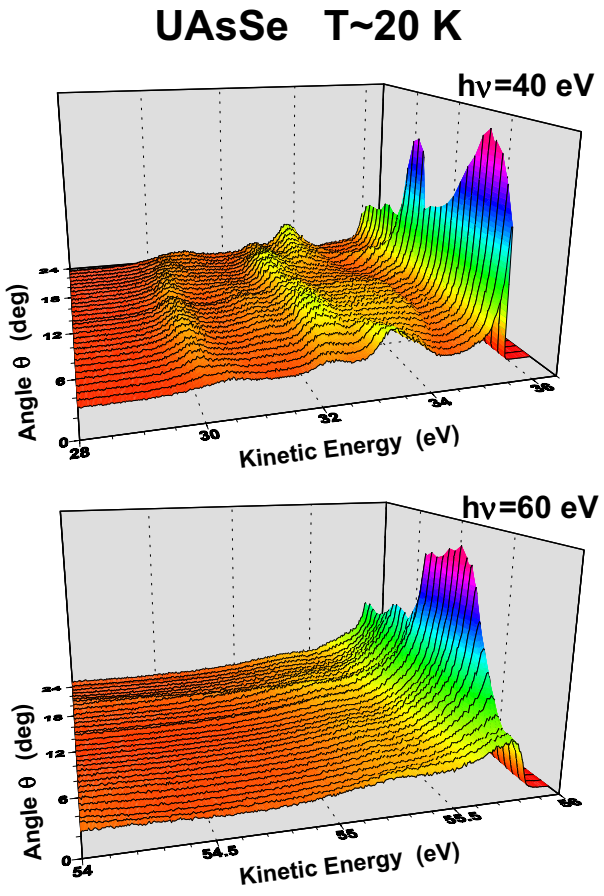

CP532, Plutonium Futures – The Science, edited by K. K. S. Pillay and K. C. Kim,
2000 American Institute of Physics 1-56396-948-3

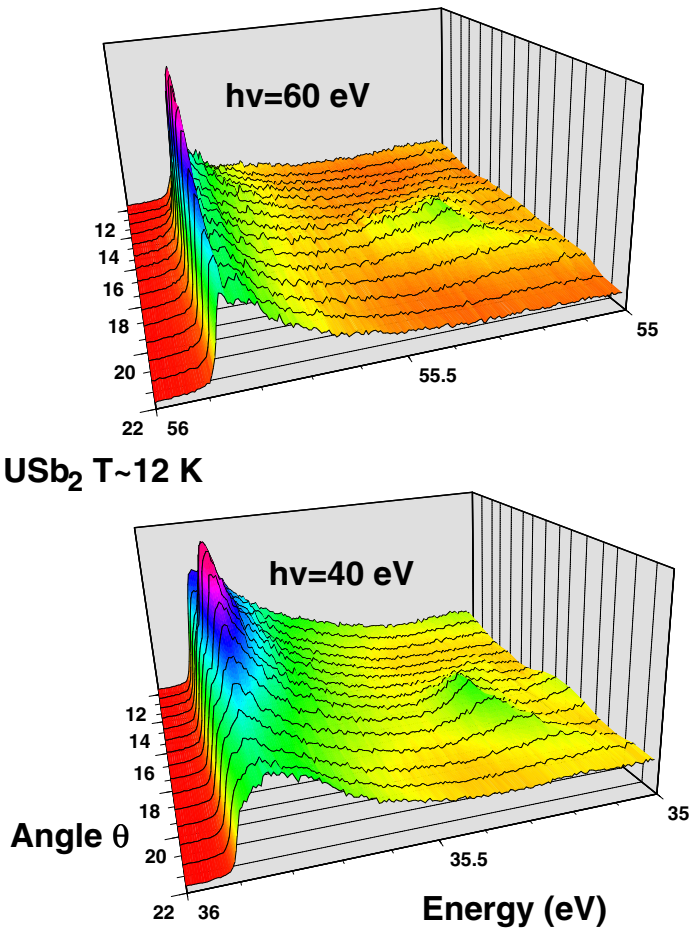

The heavy fermion material UPt_3 behaves in an entirely similar fashion, though the data in that material were acquired on a less precise apparatus. Thus it would appear that the itinerant nature of 5f electrons in even strongly correlated uranium systems is well established, and we must look for for an alternative to the single impurity model.

All-Electron Density Functional Theory Calculations of the Zero-Pressure Properties of Plutonium Dioxide

Jonathan C. Boettger
Los Alamos National Laboratory, Los Alamos, NM 87545, USA

Asok K. Ray
University of Texas, Arlington, TX 76019, USA

The fluorite structure light-actinide dioxides, uranium dioxide and plutonium dioxide, are both known to be prototypical Mott-Hubbard insulators, with band gaps produced by strong Coulomb correlation effects that are not adequately accounted for in traditional density functional theory (DFT) calculations. Indeed, DFT electronic structure calculations for these two actinide dioxides have been shown to incorrectly predict metallic behavior.[1] The highly-correlated electron effects exhibited by the actinide dioxides, combined with the large relativistic effects (including spin-orbit coupling) expected for any actinide compound, provide an extreme challenge for electronic structure theorists. For this reason, few fully-self-consistent DFT calculations have been carried out for the actinide dioxides, in general, and only one for plutonium dioxide.[1] In that calculation, the troublesome 5f electrons were treated as core electrons, and spin-orbit coupling was ignored.

In this investigation, a relativistic variant of the linear combinations of Gaussian type orbitals - fitting function (LCGTO-FF) technique has been used to carry out all-electron, full-potential, DFT electronic structure calculations on the properties of plutonium dioxide. In particular, the effects of several common approximations have been examined closely: scalar-relativity (SR) vs. full-relativity (FR); non-spin-polarized (NSP) vs. spin-polarized (SP); and local density approximation (LDA) vs. generalized gradient approximation (GGA). (Similar work was recently carried out for uranium dioxide.[2]) To this end, NSP LDA and GGA calculations were carried out at both the SR and FR levels of approximation. Then, SP calculations were carried out for the presumptively more accurate GGA model, without spin-orbit coupling included (the program used here does not yet allow simultaneous SP and spin-orbit coupling). When those SP calculations were initiated with a small ferromagnetic moment, that moment rapidly converged to 4 spins per plutonium ion, indicating that all four Pu(5f) electrons were aligned.

The present calculations incorrectly predict that plutonium dioxide is a metal for each combination of approximations considered, as expected for a Mott-Hubbard insulator. Although this qualitative failure renders any detailed analysis of the one-electron properties meaningless, the calculations do provide insight into the relative importance of spin-polarization and spin-orbit coupling effects. Examination of the band structures (not shown) indicates that the splitting of the Pu(5f) bands due to spin-polarization is roughly 2.4 eV. In contrast, the spin-orbit splitting of the Pu(5f) bands is only 0.5 eV. This result suggests that spin-polarization effects have a substantially larger impact on the one-electron properties of plutonium dioxide than spin-orbit coupling, although the latter effect might be required to determine fine details.

The lattice constants and bulk modulii found here for the various combinations of approximations are compared with experimental values[3] in Table I. Careful examination of the results in the table reveals that density gradient corrections, spin-polarization, and spin-orbit coupling each increase the lattice constant by 0.1 to 0.2 au, and decrease the bulk modulus by 15 to 30 GPa. Although these individual effects are small, the cummulative effect is significant. The lattice constant and bulk modulus that would be produced by a FR-SP-GGA calculation

CP532, Plutonium Futures – The Science, edited by K. K. S. Pillay and K. C. Kim,
2000 American Institute of Physics 1-56396-948-3

have been estimated in the table under the assumption that spin-orbit coupling has the same effect on the SP-GGA results as on the NSP-GGA results. The lattice constant estimated for the FR-SP-GGA approximation is in good agreement with experiment given the known tendency of the GGA to slightly overestimate lattice constants. On the other hand, the bulk modulus for plutonium dioxide is drastically underestimated for all of the approximations considered here. This result is particularly surprising because the reverse situation occurs for metallic plutonium, with FR GGA calculations overestimating the bulk modulus by a factor of three.[4]

Model	Spin	Relativity	a (au)	B (GPa)
LDA	NSP	SR	9.83	246
LDA	NSP	FR	10.00	218
GGA	NSP	SR	10.03	220
GGA	NSP	FR	10.21	192
GGA	SP	SR	10.12	203
GGA	SP	FR	10.30	175
Experiment			10.20	379

Table I. Theoretical lattice parameters and bulk moduli obtained here for plutonium dioxide with various combinations of approximations are compared with experiment. The FR-SP-GGA results listed are estimates.

Acknowledgments

The work of JCB was supported by the U. S. Department of Energy under contract W-7405-ENG-36. Partial support for JCB was provided by the LDRD program at LANL. The work of AKR was prepared with the support of the U. S. Department of Energy, Cooperative Agreement No. DE-FC04 95AL85832. The work of AKR was conducted through the Amarillo National Research Center.

References

1. P. J. Kelly and M. S. S. Brooks, J. Chem. Soc., Faraday Trans. **83**, 1189 (1987).

2. J. C. Boettger and A. K. Ray, Internat. J. Quantum Chem. (submitted).

3. U. Benedict, G. D. Andreetti, J. M. Fournier, and A. Waintal, J. Physique - Lettres **43,** L171 (1982); U. Benedict and W. B. Holzapfel, Handbook on the Physics and Chemistry of Rare Earths **17**, 245 (1993); and references therein.

4. M. D. Jones, J. C. Boettger, R. C. Albers, and D. J. Singh, Phys. Rev. B **61,** 4644 (2000).

Predictions of Plutonium Alloy Phase Stability Using Electronic Properties (ms120)

D. L. Olson,
G. R. Edwards,
D. E. Dooley
Colorado School of Mines, Golden, CO 80407-1887, USA

Phase stability of plutonium alloys can be assessed by using modified empirical electronic models in conjunction with measurements of electronic and magnetic properties of plutonium alloys. Electronic and magnetic property measurements can potentially non-destructively assess alloyed plutonium phase stability and the defect structures within the microstructure. These measured physical material properties are dependent on the phases present since the electronic configuration of each phase represents a unique excited electron state. Investigators during the 60s and 70s, such as Brewer, have developed empirical models allowing for the prediction of the electronic configuration of specific phases.[1] Brewer has estimated energies of each electronic configuration for lanthanides and actinides.[2,3] Using solid solution thermodynamics in combination with these electronic models, the phase diagram for an elemental metal and dilute solid solutions can be estimated.

There is a plethora of measurements that could be used to determine the relationship between a material's phase stability and its atomistic structure. The measurements, or properties, of interest are the Seebeck (thermopower) coefficient, magnetic, and electrical conductivity. Utilizing the information of the Seebeck (thermopower) coefficient, which gives information about the filling of electronic states in the vicinity of the Brillouin zone boundary, the compositional range resulting in phase transitions can be identified. A strong deviation in the Seebeck coefficient is an indication that much higher energy states are being filled. In order for the material to minimize its energy, the material will undergo a transition to a different crystal structure (reciprocal lattice and Brillouin zone configuration) that results in the lowest energy state available. Magnetic measurements render information about the *d* and *f* electron shells. Information about these shells can be related to specific excited electronic hybrid states and thus phase crystal structure. Electrical conductivity measurements can give qualitative information on the influence of defects and microstructure features on the movement of electrons.

Combining these three property measurements (or three other phase sensitive properties) into a three-dimensional plot with each property on each axis, a region of space will be formed. This region identifies the combination of the three phase sensitive properties which result in the material having a stable phase. A schematic drawing of this concept is shown in Figure 1.

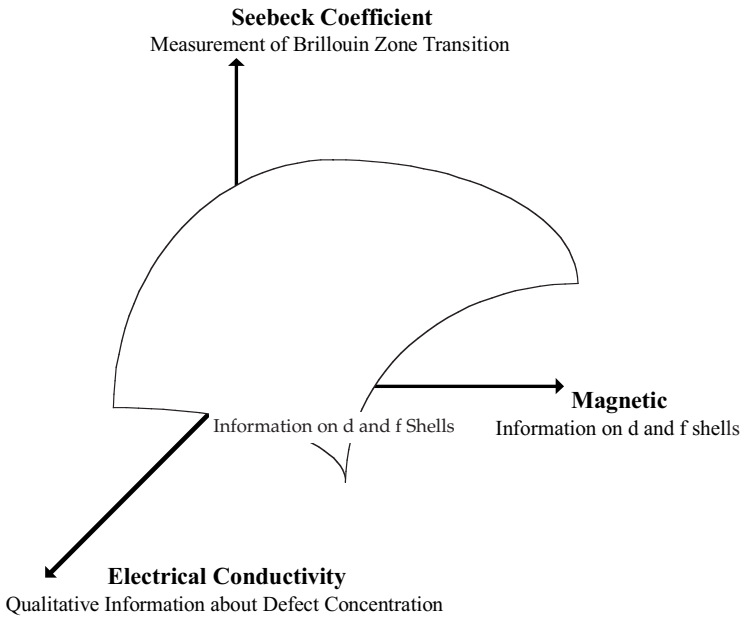

Figure 1. Zone designating a stable phase region according to these properties.

CP532, Plutonium Futures – The Science, edited by K. K. S. Pillay and K. C. Kim,

The evolution of electronic-base alloy theories as applied to the prediction of the solubility of gallium in plutonium will be presented. The necessary physical and chemical data to support predictive phase equilibrium models will be identified. The full implication of the successful use of modified empirical electronic models with thermodynamic concepts of phase diagram determination will require a team effort involving physical and chemical property analysts, solution thermodynamists, and scientists focused on the microstructural evolution of plutonium.

References

1. Hume-Rothery, W., *The Engel-Brewer Theories of Metals and Alloys*, **Progress in Materials Science**, Vol. 13, No. 5, Pergamon Press, Oxford, England, 1967.

2. Brewer, Leo, *Thermodynamics and Alloy Behavior of the BCC and FCC Phases of Plutonium and Thorium*, Plutonium 1970, TMS Nuclear Metallurgy Series, Vol. 17, Pt. 2, 1970.

3. Brewer, Leo, *Calculation of Phase Diagrams of the Actinides*, Journal of Alloys and Compounds, Vol. 213/214, pp.132, 1994.

Structural Stability in High Temperature Pu and Pu Alloys

John Wills,
Heinrich Roder
Los Alamos National Laboratory, Los Alamos, NM 87545, USA

Olof R. Eriksson
Uppsala University, Sweden

Introduction

Recent work has shown that the ground state (zero temperature) structural properties of the elemental actinides are well described by electronic structure theory using a local density or semi-local density approximation (LDA or GGA) for electron exchange and correlation. In contrast, the high temperature and alloy structures of Pu are not well understood by ab-inito theory. Accurate electronic structure calculations cannot reproduce equilibrium volumes and elastic properties of these structures and alloys, and calculated cohesive energies of the high temperature structures seem too high above the ground state to be accessible thermally.

It is generally accepted that the properties of the high-temperature phases require a reduction in bonding coming from 5f electrons, but the source of this reduction has not been determined. Strong electron correlations and localization driven by structural distortion are two of the suggestions that have been put forward. Attempts to include electron correlation beyond the local density approximation have been limited to phenomenological Hamiltonians lacking sufficient accuracy to deal with, and be tested against, real materials and structures. At the present time, the size of a unit cell necessary for a realistic study of disorder effects is prohibitively large. We have developed a model, which we call the mixed-level state, that relies only on the assumption that partial localization of the 5f manifold is responsible for the reduced bonding. The mixed-level model is quite successful in describing the basic structural properties of delta Pu and Pu-Ga stochiometric alloys.

Method

We postulate that the source of the reduction in 5f bonding is a partial localization of the 5f manifold. The localization need not be complete, so long as any hybridization between 5f sites may be regarded as a small, many-body perturbation. We may then, without deciding the cause of the localization, construct a calculational scheme which is "ab-initio" in the sense that the input consists in principal of the atomic numbers of the constituent atoms and the geometry. We realize this model by partitioning the 5f manifold into localized and itinerant parts by means of a constraint on the density functional energy. The total energy then consists of two terms, both functionals of the densities from itinerant and localized states. The first term is the discrete Fourier transform (DFT) energy of the total density, calculated in a semi-local density approximation; the second term is the difference in energy between a cooperative many-electron state (we use a Hunds rule state) and the barycenter (the average over configurations). In principal we may calculate this difference; in practice we use experimentally determined numbers. We then vary the number of electrons in the localized manifold to find the minimum energy configuration.

CP532, Plutonium Futures – The Science, edited by K. K. S. Pillay and K. C. Kim,
2000 American Institute of Physics 1-56396-948-3

Results

We have calculated the equilibrium volumes and total energies of delta Pu, Pu(3)Ga, and PuGa as a function of the occupation of the localized manifold. The energy is minimum with four 5f electrons localized in all cases, and the equlibrium volumes are close to the experimentally observed volumes. With this scheme, the delta phase is calculated to have an energy much closer to the energy of alpha Pu than with conventional calculations. We have also applied this scheme to the calculation of the tetragonal shear constant (C11-C12)/2 and find a that the lattice is stable against a tetragonal shear with a softened shear constant. Furthermore, the lowest energy crystal field state is a (non-magnetic) singlet, which would explain the lack of a moment in the delta phase. A further result of this calculational model is illustrated in Figure 1. This figure shows localized and itinerant solutions for the total energy for U, Pu, and Am. The itinerant solution is heavily favored in U, while the localized solution is heavily favored in Am; the two solutions are almost degenerate, on this scale, in Pu.

These results are promising both for potential calculational capability and for probing the physical source of localization in Pu and actinide compounds. We are currently applying this mixed-state model to the beta, gamma, and epsilon phases of Pu.

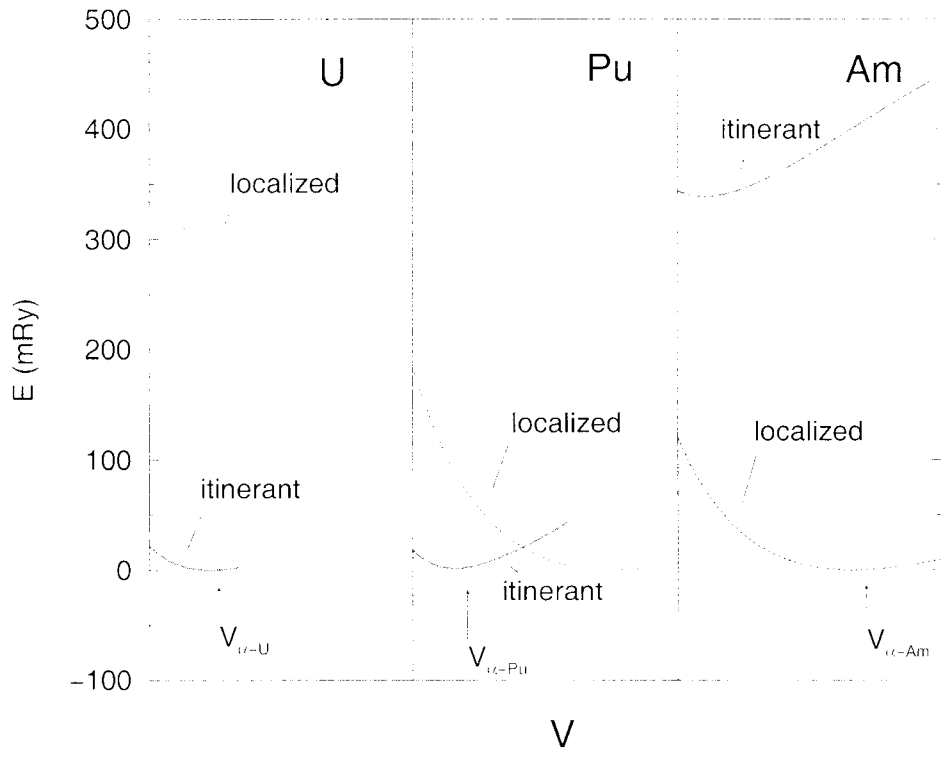

Figure 1. Itinerant and localized solutions of the total energy as a function of volume for uranium, plutonium, and americium.

Diffusion of Helium in Plutonium Alloys

D. Dooley,
B. Martinez,
D. Olson,
D. Olivas,
R. Ronquillo,
T. Rising
Los Alamos National Laboratory, Los Alamos, NM 87545, USA

Since nuclear underground testing ceased in 1992, reliance on scientific interpretation of aging properties of plutonium alloys has greatly increased in importance. Therefore, justifications of reliability of plutonium alloys must be based on experimental data. One area of interest where new data could have a significant impact is the determination of the behavior of helium in plutonium alloys.

Helium is not naturally present in materials. To study the behavior of helium in materials, helium must be introduced into the crystal lattice by bombardment, by implantation, or by nuclear decay. Helium is introduced into the plutonium lattice by nuclear decay (alpha decay).

$$^{239}Pu \rightarrow ^{235}U + ^{4}He$$

Figure 1 shows the relative amount of helium that is produced over time from the decay of plutonium for typical weapons compositions.

Many interactions occur when plutonium decays into uranium and an alpha particle. On average, the total amount of energy released from a plutonium alpha decay event is 5.24 MeV. Conservation of momentum dictates that the uranium atom and alpha particle will have an average energy of 0.09 and 5.15 MeV, respectively. This amount of energy must be dissipated, which generates many different types of interaction between the plutonium atoms, the uranium atoms, and the helium atoms. There are a number of helium interactions occurring in a lattice. Helium interactions include (1) trapping and thermal detrapping of helium in single vacancies, divacancies, and higher order clusters; (2) helium trapping at dislocations and grain boundaries; (3) replacement of helium bound to single vacancies by either interstitial plutonium atoms or uranium atoms; (4) helium clustering into vacancy-helium complexes; (5) displacement of trapped helium atoms by helium-helium or helium-uranium collisions; and (6) diffusion of helium as an interstitial.[1]

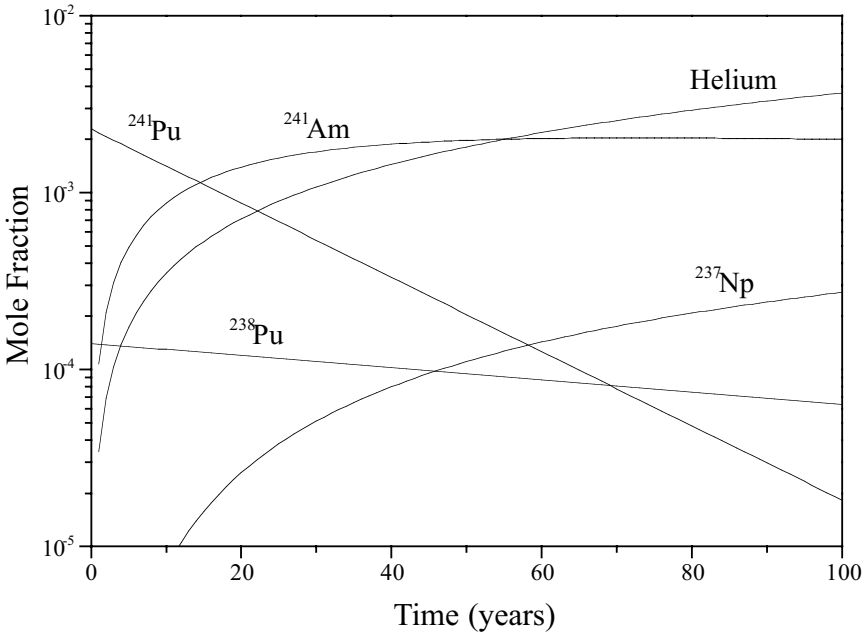

Figure 1. Decay of plutonium and production of its daughter products.

CP532, Plutonium Futures – The Science, edited by K. K. S. Pillay and K. C. Kim,
2000 American Institute of Physics 1-56396-948-3

Past research shows the presence of helium can significantly alter the behavior of metals and alloys[2,3,4,5,6] because helium is essentially insoluble in metals.[7] Theoretical calculations show that when helium occupies interstitial positions, it has the ability to move through the lattice at a significant rate.[8] Also, calculations show that helium atoms in nickel and copper energetically prefer to cluster rather than remain as isolated interstitial atoms.[9] Helium atoms will cluster at defects such as vacancies, dislocations, or grain boundaries. Finally, atomistic calculations are able to verify the observation that helium, however introduced into the lattice, will remain trapped until thermally desorbed.[10,11,12]

As the U.S. stockpile of nuclear weapons ages, it is important that we quantify and determine the effects of helium accumulation in the plutonium-239 crystal lattice. One way to characterize aging effects in plutonium is to accelerate aging by doping plutonium-239 with plutonium-238 because plutonium-238 decays approximately 282 times faster than plutonium-239. The time-dependent phenomena we expect to simulate by plutonium-238 doping are radiation-induced void formation and swelling; ingrowth of helium, uranium, and americium; and phase stability.

We are preparing plutonium-239 metal blended with 5% and 7.5% plutonium-238. Referencing the yearly total amount of helium produced from plutonium and uranium decay, 5% and 7.5% plutonium-238 ages approximately 12 and 17 times faster than electrorefined plutonium each year, respectively. Figure 2 shows the influence of increasing the concentration of plutonium-238 on simulating the real-time aged alloys.

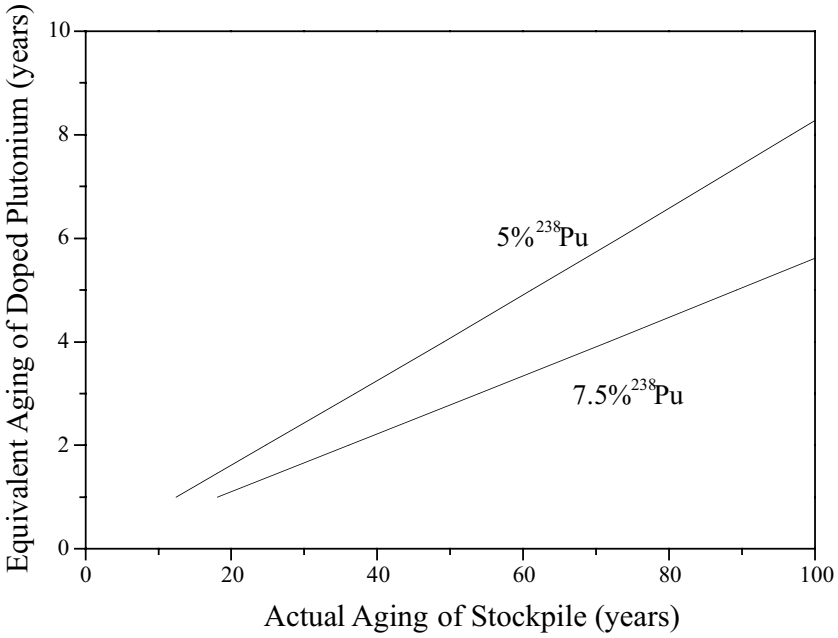

Figure 2. Equivalent ages for doped plutonium and actual plutonium.

We alloyed the doped plutonium metal with gallium to produce a solute-stabilized delta phase. Samples of this alloy are stored under carefully controlled conditions designed to simulate realistic stockpile storage environments, accounting for self-heating and thermally sensitive aging effects. We will perform periodic measurements of the kinetics of helium effusion in the doped alloys and compare

the results to those for undoped cast material and samples from aged undoped plutonium. The data can then be used to estimate the locations where helium is being trapped.

We use a Sieverts equilibrium system to perform thermal desorption experiments. The apparatus consists of a furnace connected to a manifold with volumes precisely calibrated as a function of temperature. A mass spectrometer is used to determine exact ratios of helium gas collected from the samples. Preliminary helium effusion data are presented for accelerated aged and real-time aged material.

References

1. N. M. Ghoniem, S. Sharafat, J. M. Williams, L. K. Mansur, *Journal of Nuclear Materials*, Vol. 117, 1983, pp. 96.

2. H. Ullmaier, *Nuclear Fusion*, Vol. 24, 1984, pp. 1503.

3. K. Farrell, *Radiation Effects*, Vol. 53, 1980, pp. 175.

4. G. R. Odette, P. J. Maziasz, and J. A. Spitznagel, *Journal of Nuclear Materials*, Vol. 103 and 104, 1981, pp. 1289.

5. K. Farrell, P. J. Maziasz, E. H. Lee, and L. K. Mansur, *Radiation Effects*, Vol. 78, 1983, pp. 277.

6. H. Schroeder and P. Batfalsky, *Journal of Nuclear Materials*, Vol. 103 and 104, 1981, pp. 839.

7. S. M. Murphy, *Radiation-Induced Changed in Microstructure: 13th International Symposium*, ASTM STP 955, F. A. Garner, N. H. Packan, and A. S. Kumar, Eds., American Society for Testing and Materials, Philidelphia, 1987, pp. 330.

8. M. I. Baskes and C. F. Melius, *Physical Review B*, Vol. 20, 1979, pp. 3197.

9. M. I. Baskes and W. D. Wilson, *Physical Review B*, Vol. 27, No 4, pp. 2210.

10. E. V. Kornelsen, *Canadian Journal of Physics*, Vol. 48, 1970, pp. 2812.

11. E. V. Kornelsen, *Radiation Effects*, Vol. 13, 1972, pp. 227.

12. E .V. Kornelsen and A. A. van Gorkum, *Journal of Nuclear Materials*, Vol. 92, 1980, pp. 79.

Effects of Self-Irradiated Damage on Physical Properties of Stabilized Pu Alloys

F. Freibert,
B. Martinez,
J. P. Baiardo,
J. Olivas,
R. Ronquillo
Los Alamos National Laboratory, Los Alamos, NM 87545, USA

Introduction

Our team is currently conducting experiments in the areas of thermal, physical and magnetic properties of Pu^{239} alloys doped with small quantities of Pu^{238} in an effort to further our understanding of alterations in electronic structure and self-irradiated damage in these alloys. The combination of data from these measurements will provide the following information: elastic properties and material compressibility, relative lattice defect concentration, microstructure alterations and phase homogeneity, phase transition onset temperature, intermediate phase stability, and transformation type. This series of measurements will provide a unique before and after picture of aging in these stabilized alloys, therefore answering important questions concerning these materials and providing valuable comparisons between newly cast materials and site-returned materials.

Experimental Work

We will apply these solid state experimental capabilities to determine the reversible and irreversible thermodynamics of these Pu alloys. Since thermodynamics controls alloying, homogeneity, and long-term phase stability, these studies will provide a sound technical and scientific foundation for understanding self–irradiation damage within these materials. In the case of Pu, self-irradiation damage is the result of a decay process in which an a-particle and a recoiling U atom release decay energy into the lattice through successive collisions. These collisions result in lattice defect and thermal energy production.

Past and present studies of Pu self-irradiation damage[1] have been dependent upon the addition of small quantities of the more radioactive Pu^{238} isotope to Pu^{239}. These defects are mobile at ambient temperature, so the samples should be stored at cryogenic temperatures if the full spectrum of defects can be retained within the structure and studied. This behavior represents the time accumulation of scattering sources as detected by electrical resistivity in doped and undoped samples of α-phase Pu maintained at 22.5K.[2] This self –irradiation damage can be removed by annealing the samples at higher temperatures, and the damage removal mechanism operates in stages.[2]

Both conduction electrons and phonons are well described as waves within crystalline solids, and so both are susceptible to scattering from impurities, defects, lattice instabilities, spin waves, etc. These electrons and phonons transport thermal and electric energy through the solid according to irreversible thermodynamics.[3] Electrical resistivity (r) originates from the scattering of the electron current as it flows through the solid under a motivating electrical voltage. Thermal Conductivity (k) originates from the additive response of electrons and phonons as they flow through the solid under a motivating temperature gradient. In metals, the quantity rk/T has a constant value known as the Lorentz number $L_o=2.4\times10^{-9}(V/K)^2$, which is a direct indicator of electronic scattering with phonons. Variations from this constant value indicate scattering that results from dynamic instabilities in the lattice, ionized impurities, and other scattering

CP532, Plutonium Futures – The Science, edited by K. K. S. Pillay and K. C. Kim,
2000 American Institute of Physics 1-56396-948-3

sources. Thermoelectric power (a) is the most sensitive transport property, because it is strongly dependent on the number of electrons for scattering and changes in the mean free path between scattering events. The sign of the thermoelectric power is a direct measure of the dominant carrier, either electrons or holes, and is sensitive to magnetic impurities within the metal, which can be correlated with magnetic susceptibility measurements.

Reversible thermodynamics is also being utilized in this study. Dilatometry and resonance ultrasound spectroscopy (RUS) are useful in determining the anharmonic and elastic nature of the inter-atomic bonding properties of a solid, respectively, and so easily detect changes in bonding between atoms associated with crystal symmetry changes, alterations in the unit cell volume, and lattice damage. AC/DC magnetic susceptibility is determined by the magnetic response of a material to low frequency and/or constant magnetic fields and establishes the magnetic response of the material, the existence of magnetic impurities and the clustering of these impurities into magnetic domains.

References

1. M. J. Mortimer, J. A. C. Marples, and J. A. Lee, *International Metallurgical Reviews*, **20**, 109 (1975).

2. R. O. Elliot and C. E. Olsen, *J. Appl. Phys.*, **35**, 1925 (1964).

3. H. B. Callen, *Thermodynamics and an Introduction to Thermostatistics*, Wiley: New York (1985).

Author Index

D

E

F

G

H

I

J

K

L

M

N

O

P

Q

R

S

T

V

W

X

Y

Z

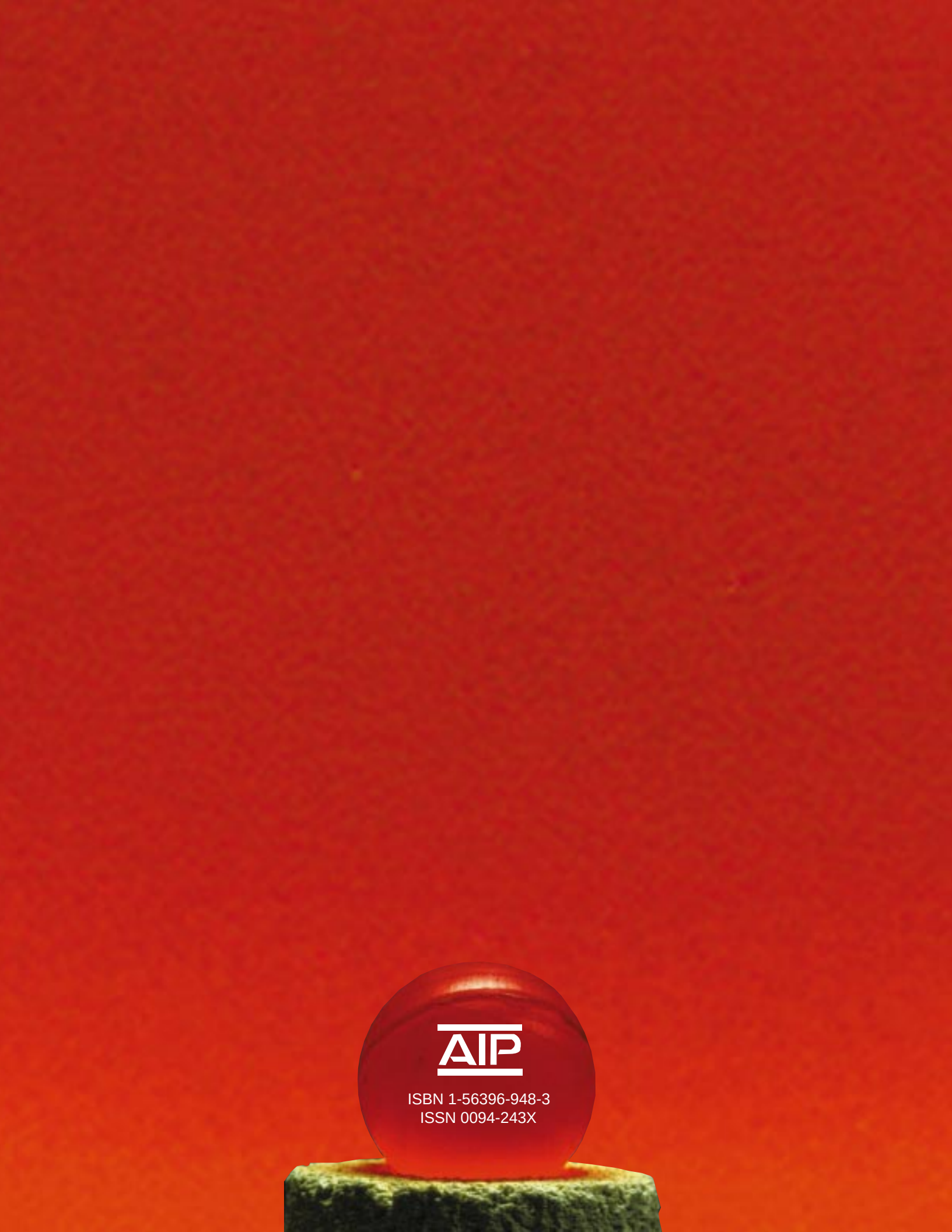

ISBN 1-56396-948-3
ISSN 0094-243X